ISSN 1674-1056
http://cpb.iphy.ac.cn
http://iopscience.iop.org/cpb
中国物理 B
Chinese Physics
中国物理 Chinese Physics B

Exploration and elaboration of photo-induced proton transfer dynamical mechanism for novel 2-[1,3]dithian-2-yl-6-(7aH-indol-2-yl)-phenol sensor

Lei Xu(许磊), Tian-Jie Zhang(张天杰), Qiao-Li Zhang(张巧丽), Da-Peng Yang(杨大鹏)
Citation: Chin. Phys. B . 2020, 29(5): 053102 . **doi:** 10.1088/1674-1056/ab8208
Journal homepage: http://cpb.iphy.ac.cn; http://iopscience.iop.org/cpb

What follows is a list of articles you may be interested in

Ab initio investigation of excited state dual hydrogen bonding interactions and proton transfer mechanism for novel oxazoline compound

Yu-Sheng Wang(王玉生), Min Jia(贾敏), Qiao-Li Zhang(张巧丽), Xiao-Yan Song(宋晓燕), Da-Peng Yang(杨大鹏)
Chin. Phys. B . 2019, 28(10): 103105 . **doi:** 10.1088/1674-1056/ab4042

The substituent effect on the excited state intramolecular proton transfer of 3-hydroxychromone

Yuzhi Song(宋玉志), Songsong Liu(刘松松), Jiajun Lu(陆佳骏), Hui Zhang(张慧), Changzhe Zhang(张常哲), Jun Du(杜军)
Chin. Phys. B . 2019, 28(9): 093102 . **doi:** 10.1088/1674-1056/ab3434

Low-lying electronic states of aluminum monoiodide

Xiang Yuan(袁翔), Shuang Yin(阴爽), Yi Lian(连艺), Pei-Yuan Yan(颜培源), Hai-Feng Xu(徐海峰), Bing Yan(闫冰)
Chin. Phys. B . 2019, 28(4): 043101 . **doi:** 10.1088/1674-1056/28/4/043101

Excited state intramolecular proton transfer mechanism of o-hydroxynaphthyl phenanthroimidazole

Shuang Liu(刘爽), Yan-Zhen Ma(马艳珍), Yun-Fan Yang(杨云帆), Song-Song Liu(刘松松), Yong-Qing Li(李永庆), Yu-Zhi Song(宋玉志)
Chin. Phys. B . 2018, 27(2): 023103 . **doi:** 10.1088/1674-1056/27/2/023103

Potential energy curves, transition dipole moments, and radiative lifetimes of KBe molecule

Ming-Jie Wan(万明杰), Cheng-Guo Jin(金成国), You Yu(虞游), Duo-Hui Huang(黄多辉), Ju-Xiang Shao(邵菊香)
Chin. Phys. B . 2017, 26(3): 033101 . **doi:** 10.1088/1674-1056/26/3/033101

Exploration and elaboration of photo-induced proton transfer dynamical mechanism for novel 2-[1,3]dithian-2-yl-6-(7aH-indol-2-yl)-phenol sensor*

Lei Xu(许磊)[1], Tian-Jie Zhang(张天杰)[1], Qiao-Li Zhang(张巧丽)[1], and Da-Peng Yang(杨大鹏)[1,2,†]

[1] School of Physics and Electronics, North China University of Water Resources and Electronic Power, Zhengzhou 450046, China
[2] Collaborative Innovation Center of Light Manipulations and Applications, Shandong Normal University, Jinan 250358, China

(Received 12 January 2020; revised manuscript received 23 February 2020; accepted manuscript online 23 March 2020)

In this work, we theoretically probe into the photo-induced hydrogen bonding effects between S0 state and S1 state as well as the excited state intramolecular proton transfer (ESIPT) behavior for a novel 2-[1,3]dithian-2-yl-6-(7 aH-indol-2-yl)-phenol (DIP) probe system. We first study the ground-state hydrogen bonding O–H···N behavior for DIP. Then we analyze the primary geometrical parameters (*i.e.*, bond length, bond angle, and infrared (IR) stretching vibrational mode) involved in hydrogen bond, and confirm that the O–H···N of DIP should be strengthened in the first excited state. It is the significant prerequisite for ESIPT reaction. Combining the frontier molecular orbitals (MOs) with vertical excitation analyses, the intramolecular charge transfer (ICT) phenomenon can be found for the DIP system, which reveals that the charge redistribution facilitates ESIPT behavior. By constructing potential energy curves for DIP along the ESIPT reactional orientation, we obtain quite a small energy barrier (3.33 kcal/mol) and affirmed that the DIP molecule undergoes ultrafast ESIPT process once it is excited to the S1 state and quickly transfers its proton, forming DIP-keto tautomer. That is why no fluorescence of DIP can be observed in experiment, which further reveals the ultrafast ESIPT mechanism proposed in this work.

Keywords: intramolecular charge transfer, ESIPT, molecular electrostatic potential, potential energy curves

PACS: 31.15.ee, 31.15.ae, 31.15.es **DOI:** 10.1088/1674-1056/ab8208

1. Introduction

Hydrogen bonds are ubiquitous and essential in the field of chemistry and biochemistry, and govern chemical reactions, supramolecular molecules, molecular assemblies, and life process.[1–3] The strength of hydrogen bonding depends on the electronegativity of donor atom which the hydrogen atom is connected with, and also depends on the ability to absorb the atom which the hydrogen atom interacts with through hydrogen bond. Both intramolecular and intermolecular hydrogen bonding affect the absorption and emission properties of the molecules. Often the fluorescent based probe molecule which forms intramolecular and intermolecular hydrogen bond is sensitive to the external environment. Therefore, there has become an increasing interest in generating novel hydrogen bonding sites in molecular probe and assemblies.[4–8]

As one of the most elementary processes throughout nature, proton transfer (PT) belongs to a fundamental class of chemical field taking place along with intramolecular or intermolecular hydrogen bond.[9–14] In view of the photo-excitation behavior, the photo-induced PT (*i.e.*, excited state intramolecular proton transfer (ESIPT)) has been regarded as one of most significant photochemical and photo-physical and photo-biological reactions in a variety of reactions.[15–20] Therefore, it has become one of the hotspots of experimental and theoretical researches in the field of chemistry. Due to the ground-state transient property, molecules containing ESIPT characteristics have been adopted in a variety of applications. The basic photo-physical and photo-chemical role of ESIPT is that the proton of one existing hydrogen bond transfers from the donor atom to acceptor moiety, which facilitates forming a transitory equilibration between enol configuration and keto configuration, emitting double fluorescence peaks and large Stokes shift.[21–30]

Generally, enol configuration should be photo-excited to S1-state enol* structure. Subsequently, the ESIPT happens and forms keto* structure in the S1 state. In view of the differences between enol* configuration and keto* configuration, normally, keto* configuration emits a longer wavelength fluorescence.[31–38] Therefore, the dual emission band could be detected. It covers a broad region of steady-state emission by promoting ESIPT molecules to become suitable for cell images, UV filters, white emitting OLEDs, fluorescent probes, molecular switchers, *etc*.[21–38] Therefore, it cannot be denied that dynamics of ESIPT reaction is beneficial for more novel applications in future.

Taking advantage of the modulations of fluorescence as well as the sensitivity to surrounding environment for ESIPT materials, advanced applications have been made in various novel areas as mentioned above. Recently, Chang *et al.* re-

*Project supported by the National Natural Science Foundation of China (Grant No. 11574083).
†Corresponding author. E-mail: dpyang_ncwu@163.com
© 2020 Chinese Physical Society and IOP Publishing Ltd

ported a new mercury ion probe based on the ESIPT mode.[39] Based on the classical 2-(2-hydroxyphenyl)benzoxazole and 2-(2-hydroxyphenyl)benzothiazole molecules and through the two-step reaction, the novel 2-[1,3]dithian-2-yl-6-(7 aH-indol-2-yl)-phenol (DIP) probe can be synthesized.[39] They inferred that the probe response might be due to the de-protection of dithian function in aqueous solution. Also, using smartphone as a signal-capturing device, the detection of metal ions is tested based on the DIP system. Thus, it can be seen that DIP molecule owns good prospects and potential for more novel development of probes. Before developing new purposes, the most fundamental excited state dynamical behaviors of DIP itself should be the primary one to be explored. In other words, a clear dynamical process of excited state for the DIP system could push and facilitate novel applications. To the best of our knowledge, only spectroscopic techniques containing time-resolved as well as steady-state electronic spectra could just reveal oblique aspects about molecular photochemical properties.[21–38] Up to now, previous investigations and observed phenomenon of DIP system are limited except experiment study. In view of the significance of theoretical work, we adopt the quantum chemical computational manner to study photo-induced cases relevant to hydrogen bonding interactions as well as ESIPT reaction. The ground-state investigations are based on density functional theory (DFT), and excited-state explorations are implemented by time-dependent DFT (TDDFT) method. In this work, we mainly focus our attention on configurations and chemical bond changes involved in intramolecular hydrogen bonding interactions. Moreover, all the chemical vibrations and infrared (IR) vibrational spectra, vertical excitation energy, frontier molecular orbitals (MOs), charge density and electronic density redistribution, and related ESIPT kinetic curves of DIP system are calculated to analyze the straightforward information about excited state dynamical process and ESIPT mechanism. Our simulated results show an ultrafast ESIPT behavior for DIP, which explains experimental fluorescence phenomenon.

2. Computational methods

In the present work, all the calculations about electronic structure are carried out by using the Gaussian 09 program suit.[40] The geometric optimization of DIP-enol and DIP-keto systemsare performed in the S0 state by using DFT and in the S1 state via TDDFT method. Here, we should mention that the reason why we select the TDDFT method is because it has become a very useful method to investigate the hydrogen-bonding interactions occurring in the excited states. Becke's three-parameter hybrid exchange functional with the Lee–Yang–Parr gradient-corrected correlation (B3LYP functional) and the triple-ζ valence quality with one set of polarization function (TZVP) basis set are selected in both DFT process and TDDFT process.[41–43] Any constrain is imposed on none of symmetry, bond lengths, bond angles or dihedral angles in the geometric optimization calculations. In order to evaluate the solvent effects and make them consistent with previous experimental results, acetonitrile solvent is selected through our calculations based on the polarizable continuum model (PCM) by using the integral equation formalism variant (IEFPCM).[44–46] It is worth mentioning that the IEFPCM model mitigates the computational burden of explicitly modeling solvent molecules and the specific interactions with the solute. The solvent can be treated as a constant dielectric reaction field where the charge density of the solute is projected onto a grid on the surface of a solvent cavity and polarized, depending on the value of the solvent dielectric. The resulting polarized charges on the cavity affect the charge density of the molecule, *etc*., until self-consistency is achieved.

All the local minima are confirmed by the absence of an imaginary mode in the vibrational analysis calculations. In addition, the S0- and S1-state potential energy curves are scanned by constrained optimization and frequency analyses to obtain the thermodynamic corrections in their corresponding electronic states by keeping the O–H bond length in step of 0.05 Å. Zero-point energy corrections and thermal corrections to the Gibbs free energy are also carried out according to the harmonic vibrational frequencies. Harmonic vibrational frequencies in the S0 and S1 states are determined via the diagonalization of Hessian matrix. The excited-stated Hessian matrix is obtained by the numerical differentiation of analytical gradient via central differences and default displacement of 0.02 Bohr. The infrared intensity is determined from the gradient of the dipole moment. Fine quadrature grids of size 4 are employed. The self-consistent field (SCF) convergence thresholds of the energy for both the ground state and excited state optimization are set to be 10^{-8} (default settings are 10^{-6}). Harmonic vibrational frequencies in the ground and excited state are determined by diagonalizing the Hessian matrix.

3. Results and discussion

As shown in Fig. 1, to confirm the stable configurations of DIP chromophore, we optimize the structure of DIP (*i.e*., DIP-enol) and its proton-transfer tautomer DIP-keto via B3LYP functional with TZVP basis set. For the DIP-enol molecule, we first study and verify the hydrogen bonding interactions. Our simulated electrostatic correlations of DIP-enol are shown in Fig. 2. Herein, we adopt red color to refer to the negative electrostatic potential, which reveals the acceptor site for hydrogen bond. Inversely, we adopt blue color to represent the positive electrostatic potential, which means the potential of hydrogen bonding donor. For DIP-enol molecule, it is obvious that O atom owns negative electrostatic potential (*i.e*., −0.452 a.u.) that is also very weak, while N atom owns posi-

tive electrostatic potential (*i.e.*, 0.168 a.u.). In view of the positive and negative electrical interaction, intramolecular hydrogen bonding correlations (O–H···N for DIP-enol) comes into being. Further, the simulated RDG *versus* sign(λ_2) and isosurface for DIP-enol are displayed in Fig. 3. According to the priciple previously proposed by Cohen *et al.*,[47] the spikes between −0.02 a.u. and −0.01 a.u. for DIP-enol further confirm the hydrogen bonding effect O–H···N for DIP-enol molecule.

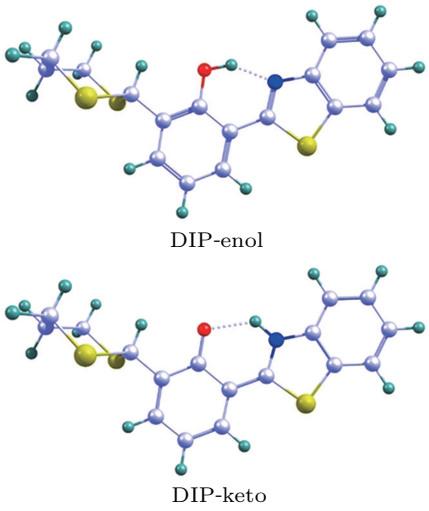


Fig. 1. Structure of DIP-enol and its proton-transfer DIP-keto tautomer.

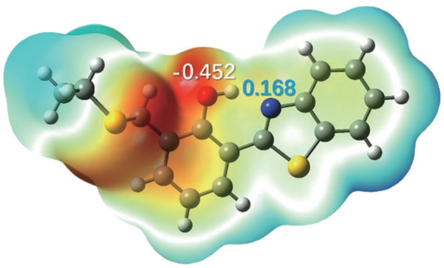


Fig. 2. Total molecular electrostatic potential for DIP-enol form.

In order to better explore the excited state dynamical behavior and ESIPT process, we first pay attention to the excited state hydrogen bonding behaviors for the DIP-enol molecule. As mentioned in previous classical work, the obtained hydrogen bond lengths, bond angles and other geometrical parameters,[48–57] and the corresponding optimized chemical bond parameters involved in intramolecular hydrogen bond O–H···N of DIP-enol compound are all listed in Table 1. Obviously, the O–H and H···N of DIP-enol are 0.995 Å and 1.704 Å in the S0 state, respectively; whereas, they change into 1.007 Å and 1.649 Å in S1 state upon photo-excitation, respectively. In other words, the lengthening of O–H bond distance and the shortening of hydrogen bond H···N (*i.e.*, from S0 to S1) indicate that the hydrogen bond O–H···N of DIP-enol is significantly enhanced in an excited state.[48–57] Furthermore, in view of bond angle ∇ (O–H···N), it is obvious that ∇ (O–H···N) also increases from 148.0° to 151.2° via the transition from S0 state to S1 state, which also verifies that the O–H···N of DIP-enol is enhanced in the S1 state.

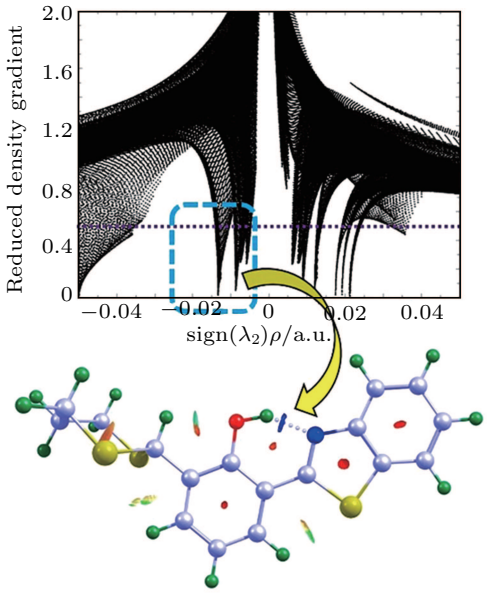


Fig. 3. Reduced density gradient (RDG) *versus* sign(λ_2) and isosurface for DIP-enol form.

Table 1. Simulated bond lengths and bond angles of DIP-enol and DIP-keto structure in S0 and S1 states, respectively.

	DIP-enol		DIP-keto	
Electronic state	S0	S1	S0	S1
O–H/Å	0.995	1.007	1.662	1.894
H–N/Å	1.704	1.649	1.048	1.023
∇ (O–H–N)/(°)	148.0	151.2	137.9	129.3

Monitoring the variations about vibrational spectral shifts is also an effective method to study the hydrogen bonding dynamics. Particularly, the vibrational spectral shifts involved in specific vibrational mode can also reflect the chemical bonding changes in excited states.[48–57] Therefore, the infrared (IR) spectra of DIP-enol compound in vibrational region of O–H stretching mode are also calculated and displayed in Fig. 4(a). Clearly, in this figure, the O–H stretching vibrational frequency is located at 3161 cm^{-1} in the S0 state. However, it largely decreases to 2917 cm^{-1} in the S1 state. In other words, the photo-excitation induces a large red-shift of 244 cm^{-1} for hydrogen bond O–H···N, which obviously reveals that the hydrogen bond in the first excited state for DIP is strengthened.[48–57] Therefore, we can drastically prove that the intramolecular hydrogen bond O–H···N of DIP-enol is largely enhanced when photo-excitation behavior occurs, which might promote the ESIPT reaction.

When we mention the photo-excitation process, we also theoretically predict the low level absorbing transitions via TDDFT/B3LYP/TZVP (*i.e*, vertical excitation energy of S_0–S_1, S_0–S_2, …, S_0–S_9) in acetonitrile solvent. Given the deactivations in high excitations, we only focus on the first excited state transition. Listed in Table 2 are the detailed results of vertical excitation energy to the low-lying single excited states for DIP-enol chemosensor. In addition, to qualitatively probe into charge and electron redistribution and charge

transfer case in excited state, we also calculate and analyze the frontier molecular orbitals (MOs) for the DIP-enol compound. According to the transition case in Table 2, the S_0–S_1 transition is the most important one due to the largest oscillator strength 0.5532. This transition refers to the transition from the highest occupied molecular orbital (HOMO) to the lowest unoccupied molecular orbital (LUMO), and these two molecular orbitals are displayed in Fig. 5. Due to the larger composition (98.14%) from HOMO to LUMO transition, we believe that the HOMO–LUMO transition dominates the S_0–S_1 transition for the DIP-enol. Obviously, the HOMO owns π characteristic, and LUMO possesses π^* property. Therefore, it can be confirmed the S_0–S_1 transition owns the $\pi\pi^*$-type character. In fact, the HOMO–LUMO transition touches on intramolecular charge transfer (ICT) peculiarity. Particularly, for the charge redistributions around hydrogen bonding moieties, the charge density of hydroxyl O atom decrease largely and that of N atom increases. In other words, the increased electronic density of proton acceptor N plays an important role in facilitating the absorption of H atoms in first excited state. Therefore, we can conclude that the orbital transition brings in more negative charges' distribution on N atom via Linus Pauling's valence-band theory. And the interaction between σ^* orbital and lone pair electrons of N facilitates ESIPT behavior for the DIP system.

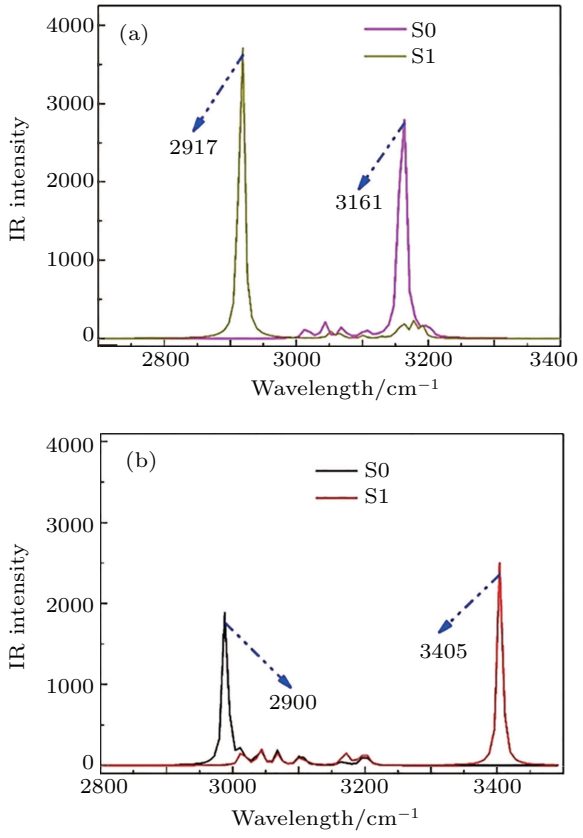


Fig. 4. Theoretical IR vibrational spectra for (a) O–H vibrational mode of DIP-enol structure and for (b) H–N vibrational mode of DIP-keto structure, in both S0 state and S1 state.

Table 2. Calculated electronic excitation energy (in unit nm), corresponding oscillator strengths and the relative compositions of the low-lying three excited states for compound DIP.

Transition	λ/nm	f	Composition	CI/%
S0 → S1	353.18	0.5532	H → L	98.41
S0 → S2	337.46	0.0622	H-1 → L	94.42
S0 → S3	317.86	0.0017	H →L+1	98.84

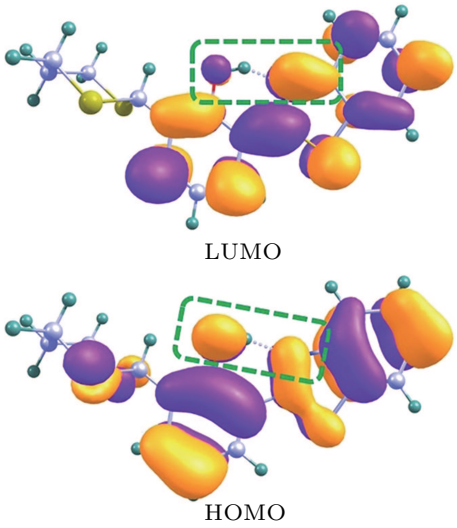


Fig. 5. Related frontier molecular orbitals (HOMO and LUMO) for DIP-enol system.

In order to clearly understand the ESIPT mechanism, the potential energy kinetic curves with O–H···N are scanned via optimization manner. To be specific, the scanning of ESIPT curves is through constrained optimization by keeping O–H bond length. Our scanned potential energy curves are shown in Fig. 6, which are obtained via only varying O–H in steps of 0.05 Å including both DIP-enol form and DIP-keto form.[58–60] For the S0-state potential energy curve, it can be clearly seen that the potential energy increases with the elongation of O–H bond, which means that the forward proton transfer from DIP-enol cannot occur thermodynamically. While for the S1-state potential energy curve, it should be noticed that the proton transfer is an ultrafast process due to the low barrier 3.3289-kcal/mol behavior. Following the ultrafast ESIPT process, the DIP-keto structure can be formed that emits fluorescence to the S0-state DIP-keto structure. By Berny optimization method, we investigate the transition state (TS) structure along the ESIPT path. The TS structure is also shown in Fig. 6. The vibrational eigenvector orientation of TS structure points to the correct ESIPT reaction direction, which confirms the ultrafast ESIPT mechanism for the DIP system. In addition, using the similar analyses to those of the IR vibrational spectra mentioned above,[48–58] we also present the IR spectra of H–N stretching mode of both S0 and S1 states in Fig. 4(b). Obviously, the S1-state H–N stretching mode of

DIP-keto structure is located at 3405 cm^{-1}, which changes to 2990 cm^{-1} in the S_0 state. That is to say, comparing with S1-state intramolecular hydrogen bond O···H–N of DIP-keto structure, this hydrogen bond should be strengthened in the S0 state due to a large redshift (415 cm^{-1}). Unquestionably, via radiation and non-radiation process, S1-state DIP-keto can be automatically de-excited to S0-state DIP-keto structure, forming more stable intramolecular hydrogen bond O···H–N. Subsequently, because of the low barrier in the ground state, the reversed ground state intramolecular proton transfer (RGSIPT) can spontaneously occur from the DIP-keto configuration to the initial DIP-enol configuration.

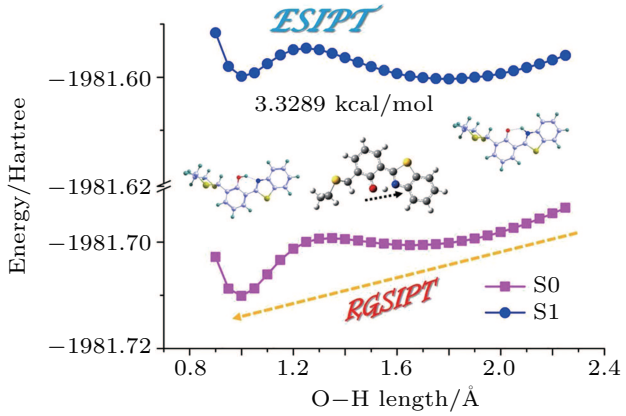


Fig. 6. PECs for DIP system via fixing O–H bond distance along intramolecular hydrogen bond O–H···N in S0 and S1 states, showing TS structure and its vibrational direction. 1 Hartree = 4.3597×10^{-18} J.

4. Conclusions

In this work, we carefully explore photo-induced hydrogen bonding dynamics and ESIPT behavior for a DIP system. The dynamics about excited state hydrogen bonding effects mainly focuses on the geometries and IR vibrational spectra. Changes of chemical parameters reveal that the hydrogen bond O–H···N of DIP should be strengthened via photo-excitation, which should be the precondition of ESIPT reaction. Furthermore, the photo-induced charge redistribution and ICT properties promote the ESIPT tendency. Particularly, the increased electronic densities around proton acceptor N moiety facilitate the absorption of hydrogen proton. The analyses about potential energy curves along the possible ESIPT path demonstrate that the ESIPT behavior of DIP system should be ultrafast due to low barrier. According to the ultrafast ESIPT mechanism, we can reasonably explain previous experiments. This work clarifies the excited state dynamical behavior for DIP system, but also fills the vacancy and inadequacy of previous experiment.

References

[1] Zhang S G 2003 *Nat. Biotechnol* **21** 1171
[2] Basabe-Desmonts L, Reinhoudt D and Crego-Calama M 2007 *Chem. Soc. Rev.* **36** 993
[3] Riel A M S, Decato D A, Sun J Y, Massena C J, Jessop M J and Berryman O B 2018 *Chem. Sci.* **9** 5828
[4] Zhang H, Wang S F, Sun Q and Smith S C 2009 *Phys. Chem. Chem. Phys.* **11** 8422
[5] Zhao G J, Northrop B H, Stang P J and Han K L 2010 *J. Phys. Chem. A* **114** 3418
[6] Liu J J, Hamza A and Zhan C G 2009 *J. Am. Chem. Soc.* **131** 11964
[7] Suh S B, Kim J C, Choi Y C, Yun S and Kim K S 2004 *J. Am. Chem. Soc.* **126** 2186
[8] Zhao G J and Han K L 2012 *Acc. Chem. Res.* **45** 404
[9] Tang K C, Chen C L, Chuang H H, Chen J L, Chen Y J, Lin Y C, Shen J Y, Hu W P and Chou P T 2011 *J. Phys. Chem. Lett.* **2** 3063
[10] Song Y Z, Liu S, Yang Y F, Wei D M, Pan J and Li Y Q 2019 *Spectrochim. Acta Part. A* **208** 309
[11] Chen C L, Tseng H W, Chen Y A, Liu J Q, Chao C M, Liu K M, Lin T C, Hung C H, Chou Y L, Lin T C and Chou P T 2016 *J. Phys. Chem. A* **120** 1020
[12] Liu S S, Zhao Y, Zhang C Z, Lin L L, Li Y Q and Song Y Z 2019 *Spectrochim. Acta Part. A* **219** 164
[13] Ma H P, Liu N and Huang J D 2017 *Sci. Rep.* **7** 331
[14] Liu S, Ma Y Z, Yang Y F, Liu S S, Li Y Q and Song Y Z 2018 *Chin. Phys. B* **27** 023103
[15] Zhao J F, Chen J S, Liu J Y and Hoffmann M R 2015 *Phys. Chem. Chem. Phys.* **17** 11990
[16] Huang J D and Ma H P 2018 *Org. Chem. Front* **5** 2749
[17] Zhao J F, Chen J S, Cui Y L, Wang J, Xia L X, Dai Y M, Song P and Ma F C 2015 *Phys. Chem. Chem. Phys.* **17** 1142
[18] Li Y O, Yang Y F and Ding Y 2017 *Sci. Rep.* **7** 1574
[19] Ma H P, Chai S, Chen D Y and Huang J D 2017 *IUCrJ.* **4** 695
[20] Li J, Li X D, Cheng S B, Song P and Zhao J F 2018 *J. At. Mol. Sci.* **9** 1
[21] Song P, Guan B J, Zhou Q, Zhao M Y, Huang J D and Ma F C 2016 *Sci. Rep.* **6** 35555
[22] Song Y Z, Liu S S, Lu J J, Zhang H, Zhang C Z and Du J 2019 *Chin. Phys. B* **28** 093102
[23] Yang D P, Zhao J F, Jia M and Song X Y 2017 *RSC Adv.* **7** 34034
[24] Huang J D, Zhao J F, Yu K, Huang X H, Cheng S B and Ma H P 2018 *Acta Crystallorgr. B* **74** 705
[25] Song Y Z, Liu S, Ma Y Z, Yang Y F, Li Y Q and Xu J H 2018 *J. Mol. Struct.* **1173** 341
[26] Zhao J F, Yao H, Liu J Y and Hoffmann M R 2015 *J. Phys. Chem. A* **119** 681
[27] Wang L F, Wang Y, Zhao J and Zhao J F 2019 *J. Phys. Org. Chem.* **32** 3954
[28] Liu S S, Pan J, Wei D M, Xu J H, Zhou Y and Song Y Z 2019 *Can. J. Phys.* **97** 721
[29] Yang D P, Li P Y, Zheng R, Wang Y S and Lv J 2016 *Theor. Chem. Acc* **135** 42
[30] Chen H, Zhao J F, Huang J D and Liang Y 2019 *Phys. Chem. Chem. Phys.* **21** 7447
[31] Zhang Q L, Yang G, Song X Y, Zhao J F and Yang D P 2018 *J. At. Mol. Sci.* **9** 7
[32] Lu X M, Zhai Y C, Zhang M X and Song Y Z 2018 *J. Phys. Org. Chem.* **31** 3821
[33] Yi J C and Fang H 2018 *Struct. Chem.* **29** 1341
[34] Zhao J F, Dong H, Yang H and Zheng Y J 2018 *Org. Chem. Front.* **5** 2710
[35] Yang D P, Zhao J F, Yang G, Song N H, Zheng R and Wang Y S 2017 *J. Mol. Liq* **241** 1003
[36] Li H, Ma L N, Yin H and Shi Y 2018 *Chin. Phys. B* **27** 098201
[37] Ni M and Fang H 2019 *Chem. Papers* **73** 1561
[38] Yi J C and Fang H 2017 *J. Mol. Model* **23** 312
[39] Chang I J, Hwang K S and Chang S K 2017 *Dyes Pigm.* **137** 69
[40] Frisch, M J, *et al*. 2009 *Gaussian* 09 Revision D. 01 Gaussian, Inc, Wallingford CT
[41] Lee C, Yang W T and Parr R G 1988 *Phys. Rev. B* **37** 785
[42] Kolth W, Becke A D and Parr R G 1996 *J. Phys. Chem.* **100** 12974
[43] Feller D 1996 *J. Comput. Chem.* **17** 1571
[44] Mennucci B, Cances E and Tomasi J 1997 *J. Phys. Chem. B* **101** 10506
[45] Cances E, Mennucci B and Tomasi J 1997 *J. Chen. Phys.* **107** 3032
[46] Cammi R and Tomasi J 1995 *J. Comput. Chem.* **16** 1449

[47] Johnson E R, Keinan S, Mori-Sanzhez P, Contreras-Garcia J, Cohen A J and Yang W T 2010 *J. Am. Chem. Soc.* **132** 6498
[48] Zhou P W, Hoffmann M, Han K L and He G Z 2015 *J. Phys. Chem. B* **119** 2125
[49] Ni M, Su S Y and Fang H 2019 *Theor. Chem. Acc.* **138** 125
[50] Xiao D, Zhang G L, Wang H Y, Tang G Q and Chen W J 2000 *Chin. Phys. Lett.* **17** 809
[51] Zhao G J and Han K L 2007 *J. Phys. Chem. A* **111** 2469
[52] Zhou P W, Li P, Zhao Y L and Han K L 2019 *J. Phys. Chem. Lett.* **10** 6929
[53] Yi J C and Fang H 2018 *Photochem. Photobiol.* **94** 27
[54] Meng Q C, Yang S Q, Ren G H and Chu T S 2018 *Chin. Phys. Lett.* **35** 098201
[55] Zhou P W and Han K L 2018 *Acc. Chem. Res.* **51** 1681
[56] Zhao G J and Han K L 2008 *J. Comput. Chem.* **29** 2010
[57] Zhao J F, Song P, Cui Y L, Liu X M, Sun S W, Hou S Y and Ma F C 2014 *Spectrochim. Acta Part. A* **131** 282
[58] Sobolewski A L and Domcke W 1999 *Phys. Chem. Chem. Phys.* **1** 3065
[59] Serrano-Andres L and Merchan M 2009 *J. Photochem. Photobiol. C* **10** 21
[60] Saga Y, Shibata Y and Tamiaki H 2010 *J. Photochem. Photobiol. C* **11** 15